International Journal of Immunopathology & Pharmacology

Original Research Article

Identification of heterogeneous subsets of aortic interleukin-17A-expressing CD4$^+$ T cells in atherosclerotic mice

International Journal of Immunopathology and Pharmacology
Volume 36: 1–12

DOI: 10.1177/03946320221117933
journals.sagepub.com/home/iji
SAGE

Guizhen Lin[1], Lei Zhang[1], Zheng Yan[1], Wei Jiang[1], Beibei Wu[1], Dongsheng Li[1] and Xiaofang Xiong[1]

Abstract

Objectives: T helper 17 (Th17) cells are involved in the inflammatory response of atherosclerosis. However, their heterogeneity in the atherosclerotic aorta remains elusive. This study was designed to identify aortic Th17 subsets. Methods: The surface markers and transcription factors of aortic interleukin-17A (IL-17A)-expressing T cells were determined by flow cytometry in an ApoE-deficient mouse atherosclerotic model. Viable aortic IL-17A-expressing T cell subsets were isolated by flow cytometry on the basis of surface markers, followed by characterizing their transcription factors by either flow cytometry or real-time RT-PCR. The effect of aortic IL-17A-expressing T cell subsets on aortic endothelial cells was determined in vitro. Results: C-X-C Motif Chemokine Receptor 3 (CXCR3), interleukin-17 receptor E (IL-17RE), CD200, and C-C Motif Chemokine Receptor 4 (CCR4) marked three subsets of aortic IL-17A-expressing T cells: CXCR3$^+$IL-17RE^{low}CD200$^+$CCR4$^-$ T cells expressing T-box protein expressed in T cells (T-bet) and interferon-gamma (IFN-γ), CXCR3$^+$IL-17RE^{low}CD200$^+$CCR4$^+$ T cells expressing T-bet but fewer IFN-γ, and CXCR3$^-$IL-17RE^{high}CD200$^+$CCR4$^+$ T cells expressing very low T-bet and no IFN-γ. Based on these markers, viable aortic Th17 cells, Th17.1 cells, and transitional Th17.1 cells were identified. Both Th17.1 cells and transitional Th17.1 cells were more proliferative than Th17 cells. Compared with Th17 cells, Th17.1 cells plus transitional Th17.1 cells induced higher expression of C-X-C motif chemokine ligand 1 (CXCL1), C-C motif chemokine ligand 2 (CCL2), C-X-C motif chemokine 5 (CXCL5), and granulocyte-macrophage colony-stimulating factor (GM-CSF) in aortic endothelial cells. Conclusion: IL-17A-expressing CD4$^+$ T cells were heterogeneous in atherosclerotic aortas.

Keywords

Atherosclerosis, T helper 17 cells, heterogeneity, inflammation, aorta

Date received: 9 April 2022; accepted: 19 July 2022

Introduction

Atherosclerosis is an inflammatory disease involving multiple cell types in arteries including the aorta.[1] Immune cells such as macrophages, dendritic cells, T cells, and B cells contribute to atherogenesis and influence plaque stabilization.[2] T cells participate in the formation of atherosclerotic lesions. Under the cues from antigen-presenting cells and microenvironmental factors, CD4$^+$

[1]The Department of Cardiology at Wuhan Third Hospital, Tongren Hospital of Wuhan University, Hubei Province, China

Corresponding author:
Xiaofang Xiong, The Department of Cardiology at Wuhan Third Hospital, Tongren Hospital of Wuhan University, 241 Pengliuyang Road, Wuchang District, Hubei Province 430060, China.
Email: xxf104622930@outlook.com

T cells differentiate into various effector subsets, including T helper 1 (Th1), T helper 2 (Th2), regulatory T cells (Tregs), and T helper 17 (Th17) cells. Th17 cells are particularly deeply involved in atherogenesis by producing interleukin-17A (IL-17A), interleukin-17F (IL-17F), interleukin-22 (IL-22), and other cytokines.[3] However, the role of Th17 cells in atherogenesis is under debate. Th17 cells have been shown to boost inflammatory response and foster atherosclerosis progression, although controversies remain,[4–6] whereas other reports suggest a plaque-stabilizing effect of IL-17A via collagen synthesis.[7] However, accumulative evidence suggests that Th17 cells are heterogeneous, comprising subpopulations with phenotypic and functional discrepancies.[8] Besides, Th17 cells undergo polarization toward Th1, Th2, Th9, Th22, and Tregs.[9] To our knowledge, the heterogeneity of Th17 cells in the atherosclerotic aorta remains elusive.

Most Th17 studies rely on detecting intracellular IL-17A by flow cytometry, making isolating viable Th17 cells impractical because cells need to be fixed and permeabilized. Recent progress in identifying Th subsets according to surface markers such as CXCR3, CCR4, and CCR6 has made enrichment of viable Th17 cells from organs and tissues possible.[10–14] Moreover, IL-17 receptor E (IL-17RE) is highly expressed on the surface of Th17 cells under different circumstances.[15–17] CD200, which is an inhibitory immune checkpoint, is also found to be a novel Th17 surface marker.[18] Therefore, Th17 cells could be recognized and enriched by discerning the expression profiles of these surface markers.

In the current study, we revealed Th17 heterogeneity by recognizing viable Th17 cells and Th1-like Th17 cells (Th17.1 cells) in the aortas of atherosclerotic ApoE$^{-/-}$ mice. Based on the expression of IL-17RE, CD200, CXCR3, and CCR4, aortic IFN-γ-expressing Th17.1 cells were separated from aortic Th17 cells. These Th17.1 cells were more potent than Th17 cells in inducing the expression of proinflammatory chemokines and cytokines in aortic endothelial cells. Therefore, for the first time, the presence of pathogenic aortic Th17.1 cells in atherosclerosis was confirmed.

Materials and methods

Murine atherosclerosis model

This confirmatory animal study was approved by the Wuhan University Animal Care and Use Committee. The experimental procedures were conducted according to the Wuhan University Guidelines for the Use of Animals and lasted for 8 months. Eight-week-old male apolipoprotein E-deficient mice (ApoE$^{-/-}$, C57BL/6J background) were purchased from Beijing Biocytogen Co., Ltd. The mice were fed a high-fat chow with 0.2% cholesterol and 21% fat by weight for 12–18 weeks. Three age- and sex-matched wild-type C57BL/6J mice were fed with a normal chow diet for 16 weeks.

Oil red O staining

The mice were euthanized by CO_2 inhalation. The aortas were taken, fixed in 4% formaldehyde, and then immersed in 5% oil red O (Beyotime Biotech) for half an hour. After three washes in deionized water, atherosclerotic lesions, that is, oil red O-positive areas along the aorta, were recorded on a Leica DM500 fluorescence microscope (Leica).

Aorta processing and aortic cell collection

Isolation of aortic cells was achieved according to published methods with minor modifications.[19,20] Briefly, mice were anesthetized with 2% halothane-oxygen, followed by perfusion with 3 mL of phosphate-buffered saline (PBS) via cardiac puncture to remove circulating blood cells. Each aorta with branches was carefully harvested and minced into fragments of about 1 mm in length. The tissue fragments were then incubated in 100 μL of digestion buffer (RPMI1640 medium containing 10% fetal calf serum [FCS], 200 U/ml collagenase XI, 500 U/ml collagenase I, 50 U/ml hyaluronidase I-s, and 100 U/ml DNase I) for half an hour in a 37°C water bath with gentle pipetting every 5 min. The digested tissues and the digestion buffer were filtered through a 40-μm cell strainer, followed by centrifugation at 250×g for 5 min. The cell pellet was suspended in 0.5 mL of ice-cold PBS for the following experiments. In some experiments, 15 aortas were pooled and digested with proportionally increased reagents. The reagents were purchased from Sigma-Aldrich. In some experiments, the cells were stimulated with 20 ng/mL phorbol ester (PMA), 1 μg/ml ionomycin, and 10 μg/mL brefeldin A (all from Beyotime Biotech) for 4 h at 37°C before further analysis.

Blood leukocyte collection

Peripheral blood was collected from the tail vein and mixed with 1 mL of 2 mM ethylenediaminetetraacetic acid-PBS. After centrifugation at 200×g for 5 min, red blood cells were lysed by suspending the cell pellet in 0.5 mL of RBC lysis buffer (Beyotime Biotech) for 5 min at room temperature. Cells were washed with 1 mL of PBS once and subjected to the same staining procedures as for aortic cells.

Flow cytometry analysis

The antibodies are listed in Table 1. For surface protein analysis, cells were incubated with PBS containing each

Table 1. Flow cytometry antibodies.

Antibody	Cat #	Clone #	Company
APC/Cyanine7 anti-mouse CD3	100221	17A2	BioLegend
Pacific blue anti-mouse CD4	100427	GK1.5	BioLegend
PE/Cyanine7 anti-mouse CD4	100421	GK1.5	BioLegend
PE anti-mouse CD8a	100707	53-6.7	BioLegend
Pacific blue anti-mouse IL-17A	506917	TC11-18H10.1	BioLegend
PE/Cyanine7 anti-mouse CD200	123817	OX-90	BioLegend
PE anti-mouse IL-17RE	141403	TW7-16B4	BioLegend
PerCP/Cyanine5.5 anti-mouse CXCR3	126513	CXCR3-173	BioLegend
PE anti-mouse CCR4	131203	2G12	BioLegend
Alexa Fluor® 647 anti-mouse IL-17RE	FAB7997R-025UG	944904	R&D Systems
FITC anti-mouse IFN-γ	505805	XMG1.2	BioLegend
FITC anti-mouse TNF-α	506303	MP6-XT22	BioLegend
FITC anti-mouse/human Ki-67	151211	11F6	BioLegend
FITC anti-mouse/human T-bet	644811	4B10	BioLegend
Alexa Fluor™ 488 anti-mouse RORγt	53-6981-82	B2D	eBioscience
FITC anti-mouse CD31	160211	W18222 B	BioLegend
APC anti-mouse CD45	157605	QA17A26	BioLegend
Biotin anti-mouse CD144	138008	BV13	BioLegend
FITC Streptavidin	405201	—	BioLegend

Table 2. Primer sequences.

Target	Forward (5' to 3')	Reverse (5' to 3')
Gata3	cctctggaggaggaacgctaat	gtttcgggtctggatgccttct
Foxp3	cctggttgtgagaaggtcttcg	tgctccagagactgcaccactt
Rorc	gtggagtttgccaagcggcttt	cctgcacattctgactaggacg
Tbx21	ccacctgttgtggtccaagttc	ccacaaacatcctgtaatggcttg
Cxcl1	tccagagcttgaaggtgttgcc	aaccaagggagcttcagggtca
Ccl2	gctacaagaggatcaccagcag	gtctggacccattccttcttgg
Cxcl5	ccgctggcatttctgttgctgt	cagggatcacctccaaattagcg
Cxcl8	gagagtgattgagagtggaccac	gagagtgattgagagtggaccac
Cdkn2b (p15 INK4B)	atcccaacgccctgaaccgct	agttgggttctgctccgtggag
Cdkn2a (P16 INK4A)	tgttgaggctagagaggatcttg	cgaatctgcaccgtagttgagc
Cdkn2c (p18 INK4C)	gtcaacgctcaaaatggatttggg	ggattagcacctctgaggagaag
Cdkn2d (p19 INK4D)	ggagctggtgcatcctgacgc	tggcaccttgcttcaggagctc
Cdkn1a (p21 WAF1/Cip1)	tcgctgtcttgcactctggtgt	ccaatctgcgcttggagtgatag
Cdkn1b (p27 KIP1)	agcagtgtccagggatgaggaa	ttcttgggcgtctgctccacag
Cdkn1c (p57 KIP2)	agctgaaggaccagcctctctc	acgtcgttcgacgccttgttct
Actinb	gatggtgaaggtcggtgtga	tgaacttgccgtgggtagag

antibody (5 μg/ml) for 20 min on ice. To detect intracellular proteins, cells were fixed with 200 μl 3% paraformaldehyde–PBS for 10 min at room temperature, followed by incubation with 1 mL of 90% methanol–PBS for 30 min on ice. Cells were then washed with PBS and stained with 200 μl of PBS containing 5 μg/ml of each antibody for 1 h at room temperature. A BD LSRII flow cytometer was used for analysis and a BD FACSAria cell sorter was used for cell sorting (both from BD Biosciences).

Real-time reverse transcription and polymerase chain reaction (RT-PCR)

RNAs were prepared using the Arcturus PicoPure RNA Isolation Kit (Thermo Fisher) by following the supplier's manual. cDNAs were made using the RevertAid First Strand cDNA Synthesis Kit (NovoBiotechnology). The TB Green Premix Ex Taq II (Takara Bio) was used for quantitative PCR on a LightCycler® 480 platform (Roche). The primers are shown in Table 2. The transcript levels of

genes of interest were first normalized to the transcript level of β-actin and then quantified by the $2^{-\Delta\Delta Ct}$ formula.

Isolation of aortic endothelial cells

Aortic cells were collected as described above. These cells were then incubated with 200 µl of PBS containing 2 µg/ml FITC-conjugated anti-mouse CD31 antibody (BioLegend) for 20 min on ice. After three washes with PBS, $CD31^+$ AECs were sorted by the BD FACSAria cell sorter.

In vitro culture

Sorted T cells and aortic endothelial cells were suspended at the cell density of 5×10^4/ml in the culture medium (RPMI1640 medium containing 10% FCS). For intracellular cytokine staining, T cells were treated with 20 ng/mL phorbol ester (PMA), 1 µg/ml ionomycin, and 10 µg/mL brefeldin A for 4 h at 37°C.

To evaluate the effect of T cells on AECs, T cells were stimulated with 20 ng/mL PMA and 1 µg/ml ionomycin for 4 h and washed with PBS once. After that, 3000 T cells and 1000 AECs were mixed in 50 µl of culture medium and seeded in each well of a 96-well V-shaped-bottom microplate. The cells were centrifuged at 200×g for 5 min and incubated for 24 h at 37°C in an incubator. At the end of the co-culture, cells were stained with 2 µg/ml APC anti-mouse CD45 antibody and biotinylated anti-mouse CD144 antibody for 20 min on ice. Cells were washed with 0.5 mL of PBS once and incubated with 2 µg/ml FITC Streptavidin for 20 min on ice. Cells were suspended in PBS and loaded onto the BD FACSAria cell sorter to sort $CD144^+$ AECs.

Statistical analysis

Every experiment was independently carried out 2 or 3 times. The data were shown as mean ± standard deviation. The Student's t-test or one-way ANOVA with post-hoc Tukey HSD test was used to compare the differences. A *p-value* < .05 was considered significant. For each experiment, the minimum mouse number necessary for attaining the statistic power of 0.8 and type I error rate of 0.05 was determined by the Animal Sample Size Calculator, which is an open tool offered by the U.S. Department of Agriculture (www.aphis.usda.gov/aphis/ourfocus/animalhealth/ceah-toolbox/animal-sample-size-calculator), based on the mean values and standard deviations acquired in preliminary tests.

Results

The phenotypes of aortic IL-17A-expressing T cell subsets based on surface and intracellular markers

We fed $ApoE^{-/-}$ mice with a high-fat diet for 16 weeks and observed atherosclerotic lesions in their aortas (Supplementary Figure 1). To characterize the phenotype of IL-17A-expressing T cells, mouse aortas were collected and dissociated with enzymes. The resultant single cells were stimulated with PMA plus ionomycin in the presence of brefeldin A for 4 h. The cells were then stained with fluorochrome-conjugated antibodies against CD3, IL-17RE, CXCR3, CD200, and CCR4, followed by intracellular staining with fluorochrome-conjugated antibodies against IL-17A, RORγt, T-bet, or IFN-γ, respectively. The whole workflow is demonstrated in Supplementary Figure 2(A). As indicated in Figure 1(A), single cells were first gated according to the forward scatter-A and forward scatter-H. Within these single cells, a $CD3^+IL\text{-}17A^+$ population was observed, suggesting the presence of IL-17A-expressing T cells. These IL-17A-expressing T cells were $CD4^+$ T cells (Supplementary Figure 3). According to the surface staining of CXCR3 and IL-17RE, IL-17A-expressing T cells were divided into two subsets: $CXCR3^+IL\text{-}17RE^{low}$ T cells and $CXCR3^-IL\text{-}17RE^{high}$ T cells. The former constituted about 15% of IL-17A-expressing T cells while the latter accounted for over 80% of IL-17A-expressing T cells (Figure 1(B)). Further analysis revealed that $CXCR3^+IL\text{-}17RE^{low}$ T cells contained two subsets: $CD200^+CCR4^-$ cells and $CD200^+CCR4^+$ T cells, as shown in Figure 1(C) and 1D. $CXCR3^-IL\text{-}17RE^{high}$ T cells were predominantly $CD200^+CCR4^+$ (Figure 1(C)). Therefore, three subsets were present in aortic IL-17A-expressing T cells: $CXCR3^+IL\text{-}17RE^{low}CD200^+CCR4^-$ T cells (hereinafter $R3^+RE^{low}200^+R4^-$), $CXCR3^+IL\text{-}17RE^{low}CD200^+CCR4^+$ T cells ($R3^+RE^{low}200^+R4^+$), and $CXCR3^-IL\text{-}17RE^{high}CD200^+CCR4^+$ T cells (hereinafter $R3^-RE^{high}$).

Evaluation of T-bet and RORγt revealed equivalent RORγt expression in the three subsets (Figure 1(E)). However, $R3^+RE^{low}200^+R4^-$ T cells and $R3^+RE^{low}200^+R4^+$ T cells expressed higher T-bet than $R3^-RE^{high}$ T cells (Figures 1(F) and (G)). Furthermore, substantial IFN-γ expression was found in $R3^+RE^{low}200^+R4^-$ T cells, while $R3^+RE^{low}200^+R4^+$ T cells expressed fewer IFN-γ and $R3^-RE^{high}$ did not express IFN-γ (Figures 1(H) and (i)). Therefore, $R3^+RE^{low}200^+R4^-$ T cells were Th17.1 cells. $R3^+RE^{low}200^+R4^+$ T cells seemed to be transitional Th17.1 cells between the Th17 stage and Th17.1 stage. $R3^-RE^{high}$ T cells were Th17 cells.

To explore the presence of these subsets in the blood, we stained circulating leukocytes with the same antibodies against relevant surface and intracellular markers. As shown in Supplementary Figure 4(A), about 2% of $CD3^+IL\text{-}17A^+$ T cells were found in circulating leukocytes. Interestingly, these cells were all $R3^-RE^{high}$ (Supplementary Figure 4(B)) with uniform RORγt expression (Supplementary Figure 4(C)). No substantial IFN-γ expression was detected in circulating IL-17A-expressing T cells (Supplementary Figure 4(D)). Therefore, these cells

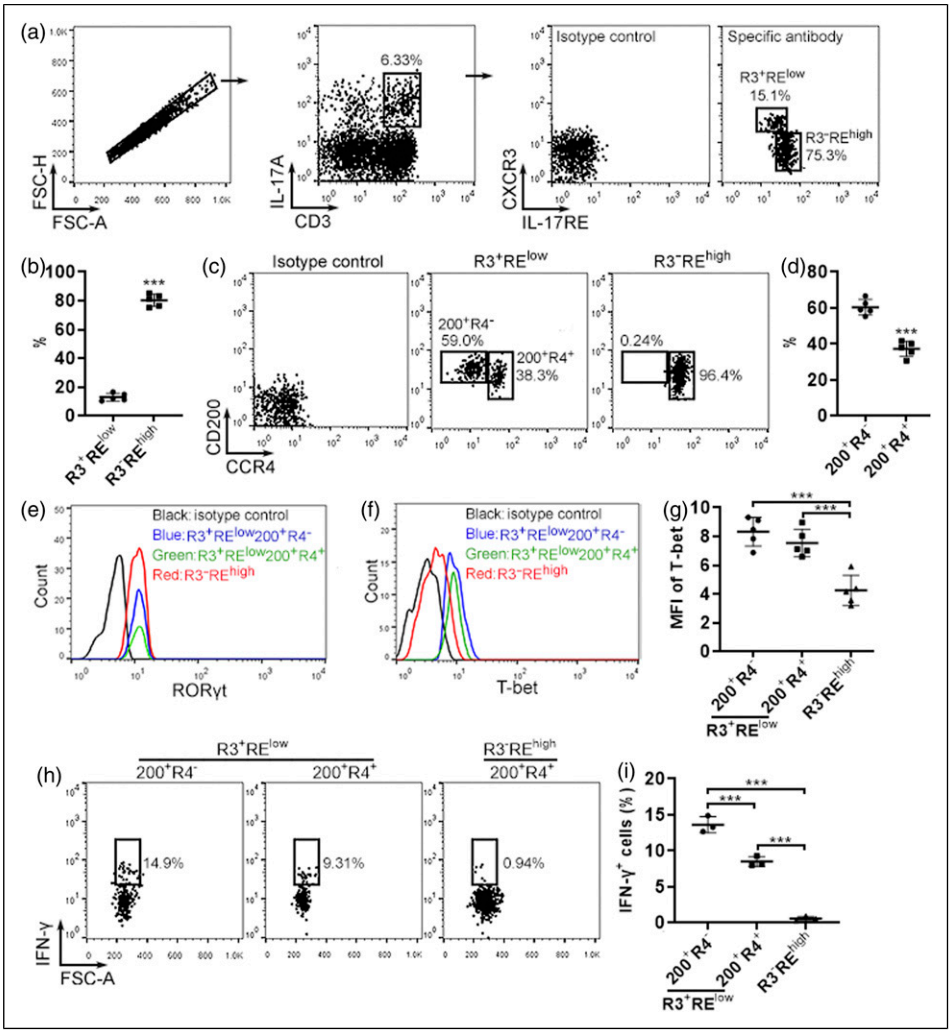

Figure 1. Phenotype of aortic IL-17A-expressing T cells. (A) Representative dot plots showing the gating strategy for aortic IL-17A-expressing T cell subsets based on CXCR3 and IL-17RE. (B) The proportions of $R3^+RE^{low}$ T cells and $R3^-RE^{high}$ T cells in total aortic IL-17A-expressing T cells. (C) Representative dot plots showing the expression of CD200 and CCR4 in $R3^+RE^{low}$ T cells and $R3^-RE^{high}$ T cells, respectively. (D) The proportions of 200^+R4^- and 200^+R4^+ cells in $R3^+RE^{low}$ T cells, respectively. (E) Representative histograms showing RORγt expression in indicated subsets. (F) Representative histograms showing T-bet protein in indicated subsets. (G) The mean fluorescence intensities (MFI) of T-bet in indicated subsets. (H) Representative dot plots showing intracellular staining of IFN-γ in indicated subsets. (I) The proportions of IFN-γ-expressing cells in indicated subsets. $N = 3$ or 5. ***: $p < .001$.

were all Th17 cells. Th17.1 and transitional Th17.1 cells were absent in the blood and were likely generated only in the atherosclerotic aorta.

Temporal changes in the frequencies of IL-17A-expressing T cell subsets

To investigate the persistence of the above-mentioned T cell subsets in the atherosclerotic aorta, we enriched aortic cells 12 weeks, 16 weeks, and 18 weeks after the high-fat diet treatment. The same staining as described above was performed to characterize the phenotype of aortic IL-17A-expressing T cells at different time points. As indicated in Figures 2(A) and (C), at week 12, the frequency of aortic IL-17A-expressing T cells was around 3.5%, and this frequency increased to over 6% at week 16 and week 18. At week 12, aortic IL-17A-expressing T cells were all $R3^-RE^{high}$ (Figures 2(A) and (D)). At week 16 and week 18, $R3^+RE^{low}$ cells emerged in aortic IL-17A-expressing T cells and increased over time (Figures 2(A) and (D)). Furthermore, at week 12, almost all aortic IL-17A-expressing T cells were 200^+R4^+. At week 16 and week 18, $R3^+RE^{low}$ T cells contained the 200^+R4^- subset and 200^+R4^+ subset. The frequency of the 200^+R4^- subset increased from week 16 to week 18, while the frequency of the 200^+R4^+ subset decreased in the same period (Figures

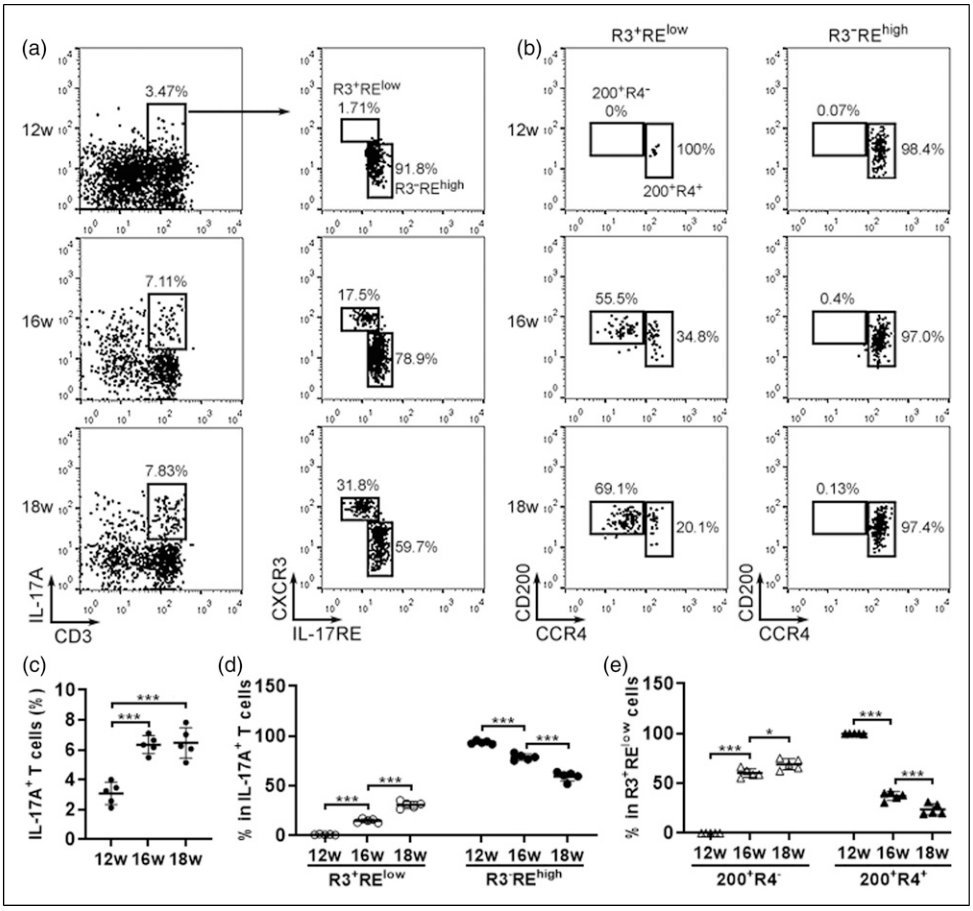

Figure 2. Temporal changes of IL-17A-expressing T cell subsets. (A) Representative dot plots showing the gating strategy for aortic IL-17A-expressing T cell subsets based on CXCR3 and IL-17RE from week 12 to week 18. (B) Representative dot plots showing the expression of CD200 and CCR4 in $R3^{+}RE^{low}$ T cells and $R3^{-}RE^{high}$ T cells. (C) The proportions of aortic IL-17A-expressing T cells in total aortic cells. (D) The proportions of $R3^{+}RE^{low}$ T cells and $R3^{-}RE^{high}$ T cells in aortic IL-17A-expressing T cells. (E) The proportions of $200^{+}R4^{-}$ and $200^{+}R4^{+}$ cells in $R3^{+}RE^{low}$ T cells at each time point. $N = 5$. *: $p < .05$. ***: $p < .001$.

2(B) and (E)). $R3^{-}RE^{high}$ T cells were constantly $200^{+}R4^{+}$ through the period tested (Figures 2(B) and (E)).

Identification of viable aortic Th17 and Th17.1 cells based on surface markers

Although the above data uncovered aortic IL-17A-expressing T cell subsets, these cells were fixed and permeabilized for intracellular IL-17A staining, making enrichment of viable Th17 and Th17.1 cells impossible. Next, we tried to identify viable Th17 and Th17.1 cells based on surface marker expression. The whole workflow is illustrated in Supplementary Figure 2(B). As indicated in Figure 3(A), $CD3^{+}CD4^{+}$ T cells were first recognized in aortic cells, and an $IL\text{-}17RE^{+}CD200^{+}$ population (hereinafter $RE^{+}200^{+}$) was found in $CD3^{+}CD4^{+}$ T cells. The rest $CD3^{+}CD4^{+}$ T cells were $IL\text{-}17RE^{-}$ (hereinafter RE^{-}). Real-time RT-PCR revealed that compared with total $CD4^{+}$ T cells, $RE^{+}200^{+}$ cells expressed higher *Rorc* mRNA and lower *Tbx21* mRNA (Figure 3(B)). No *Gata3* and *Foxp3* mRNAs were found in $RE^{+}200^{+}$ cells (Figure 3(B)). RE^{-} T cells and total $CD4^{+}$ T cells expressed equivalent *Rorc*, *Tbx21*, *Gata3*, and *Foxp3* mRNAs (Figure 3(B)). Therefore, $RE^{+}200^{+}$ cells likely contained Th17 and Th17.1 cells. Analysis of CXCR3 and CCR4 expression demonstrated three subsets in $RE^{+}200^{+}$ T cells: $CXCR3^{+}CCR4^{-}$ cells (hereinafter $R3^{+}R4^{-}$), $CXCR3^{+}CCR4^{+}$ cells (hereinafter $R3^{+}R4^{+}$), and $CXCR3^{-}CCR4^{+}$ cells (hereinafter $R3^{-}R4^{+}$) (Figure 3(C)). To identify the three subsets, they were sorted and stimulated with PMA and ionomycin for 4 h, followed by detection of intracellular RORγt, T-bet, IL-17A, IFN-γ, and TNF-α, respectively. All three subsets expressed equivalent RORγt, while $R3^{+}R4^{-}$ and $R3^{+}R4^{+}$ cells expressed higher T-bet than $R3^{-}R4^{+}$ cells (Figures 3(D) and (E)). All three subsets expressed abundant IL-17A (Figures 4(A) and (B)). Interestingly, $R3^{+}R4^{-}$ cells expressed high IFN-γ and $R3^{+}R4^{+}$ cells expressed lower IFN-γ, whereas $R3^{-}R4^{+}$ cells expressed little IFN-γ (Figures

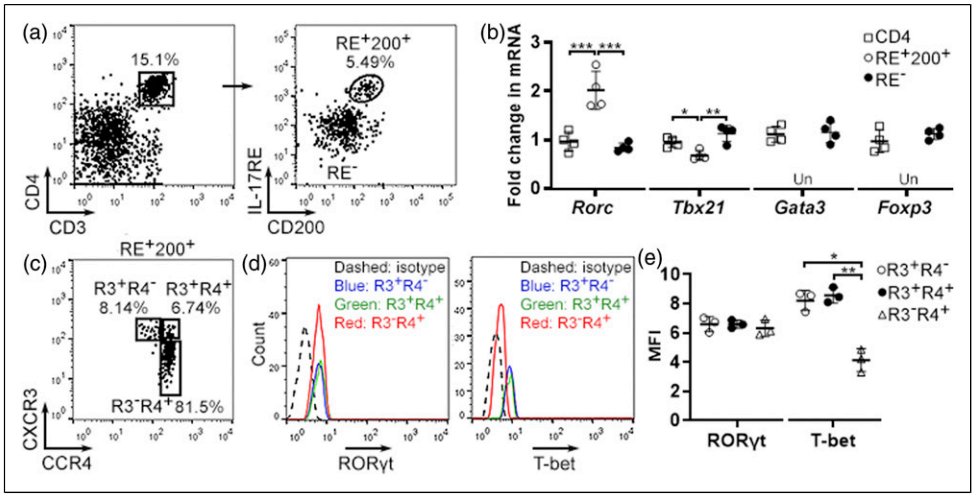

Figure 3. Recognition of viable aortic Th17 and Th17.1 cells. (A) Representative dot plots showing the gating strategy for aortic $CD3^+CD4^+RE^+CD200^+$ T cells. (B) mRNA levels of indicated transcription factors in total $CD4^+$ T cells (CD4), RE^+200^+ T cells, and RE^- T cells. Un: under detection threshold. (C) Representative dot plots showing the gating strategy for $R3^+R4^-$ cells, $R3^+R4^+$ cells, and $R3^-R4^+$ cells in aortic RE^+200^+ T cells. (D) Representative histograms showing RORγt and T-bet proteins in $R3^+R4^-$ cells, $R3^+R4^+$ cells, and $R3^-R4^+$ cells. (E) The mean fluorescence intensities (MFI) of RORγt and T-bet in the subsets. $N = 3$ or 4. *: $p < .05$. **: $p < .01$. ***: $p < .001$.

4(C) and (D)). The pattern of TNF-α expression was similar to IFN-γ (Figures 4(E) and (F)). Therefore, $R3^+R4^-$ cells were Th17.1 cells. $R3^+R4^+$ cells were transitional Th17.1 cells. $R3^-R4^+$ cells were Th17 cells.

Distinct proliferation status of aortic Th17 and Th17.1 cells

Ki67 staining of the above $R3^+R4^-$ T cells (Th17.1), $R3^+R4^+$ T cells (transitional Th17.1), and $R3^-R4^+$ T cells (Th17) indicated that the former two subsets had equivalent Ki67 expression, whereas Th17 cells expressed fewer Ki67 (Figures 5(A) and (B)). We then assessed mRNA levels of genes encoding cyclin-dependent kinase inhibitors which control cell proliferation. As indicated in Figure 5(C), the three subsets expressed comparable levels of *Cdkn2b* (p15 INK4B), *Cdkn2c* (p18 INK4C), *Cdkn2d* (p19 INK4D), and *Cdkn1c* (p57 KIP2). However, aortic Th17 cells expressed more *Cdkn2a* (P16 INK4A), *Cdkn1a* (p21 WAF1/Cip1), and *Cdkn1b* (p27 KIP1) than the other two subsets. Therefore, aortic Th17.1 cells and transitional Th17.1 cells were more proliferative than aortic Th17 cells.

The effects of aortic Th17 and Th17.1 cells on AECs

Th17 cells modulate chemokine expression in endothelial cells to facilitate leukocyte recruitment.[21,22] To check the effects of aortic Th17 and Th17.1 cells on AECs, $RE^+CD200^+R3^-R4^+$ cells (Th17 cells) and $RE^+CD200^+R3^+$ cells (i.e., combined Th17.1 and transitional Th17.1 cells, termed cTh17.1 cells hereinafter) were sorted from 15 aortas and stimulated with PMA and ionomycin. Due to their low numbers, functionally related Th17.1 cells and transitional Th17.1 cells were sorted together to prepare enough cells for the following co-culture assay. Meanwhile, mouse $CD31^+$ AECs were enriched by flow cytometry (Figure 6(A)). Stimulated Th17 cells and cTh17.1 cells were then co-cultured with AECs for 24 h at the ratio of 3:1, respectively. After that, cells were stained with a fluorochrome-conjugated anti-CD45 antibody and an anti-CD144 (VE-Cadherin) antibody. $CD144^+$ AECs were sorted from the cell mixture (Figure 6(B)) and subjected to real-time RT-PCR to analyze chemokine and cytokine mRNAs. As indicated in Figures 6(C) to (G), Th17 cells increased the mRNAs of *Cxcl1*, *Ccl2*, *Cxcl5*, and *Csf2* (GM-CSF) in AECs. Compared with Th17 cells, cTh17.1 cells induced higher expression of *Cxcl1*, *Ccl2*, *Cxcl5*, and *Csf2* in AECs. Neither Th17 cells nor cTh17.1 cells changed *Cxcl8* mRNA in AECs (Figure 6(F)). Therefore, Th17.1 and transitional Th17.1 cells might be more pro-inflammatory than Th17 cells.

Discussion

The present study characterized the phenotype of $IL\text{-}17A^+CD4^+$ T cells in the aortas of atherosclerotic mice. The logic of this study is to reveal the significant expression of CD200, IL-17RE, CXCR3, and CCR4 on the surface of aortic $IL\text{-}17A^+CD4^+$ T cells in the first place, and then distinguish viable Th17 cells according to the unique expression pattern of these surface markers. We found that aortic $IL\text{-}17A^+CD4^+$ T cells were RE^+200^+. However, the

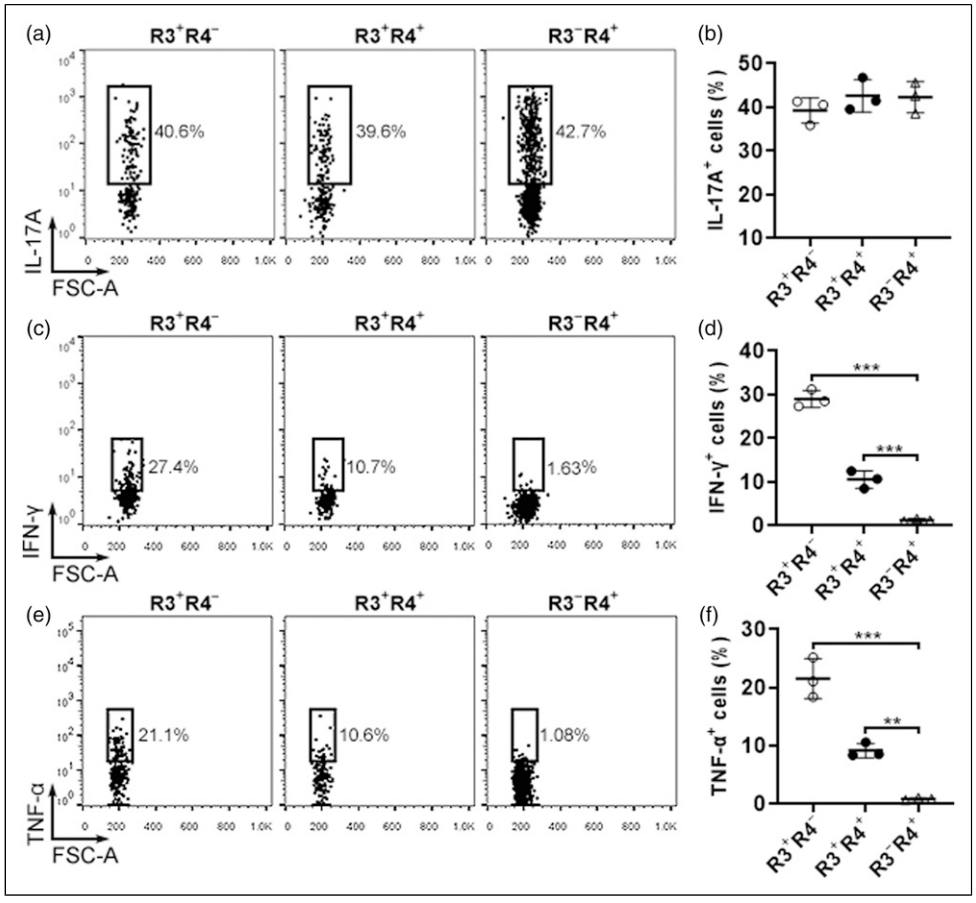

Figure 4. Expression of indicated cytokines in $R3^+R4^-$ cells, $R3^+R4^+$ cells, and $R3^-R4^+$ cells. (A, C, and E) Representative dot plots showing the expression of IL-17A (A), IFN-γ (C), and TNF-α (E) in the subsets. (B, D, and F) The proportions of IL-17A-expressing (B), IFN-γ-expressing (D), and TNF-α-expressing (F) cells in each subset, respectively. $N = 3$. **: $p < .01$. ***: $p < .001$.

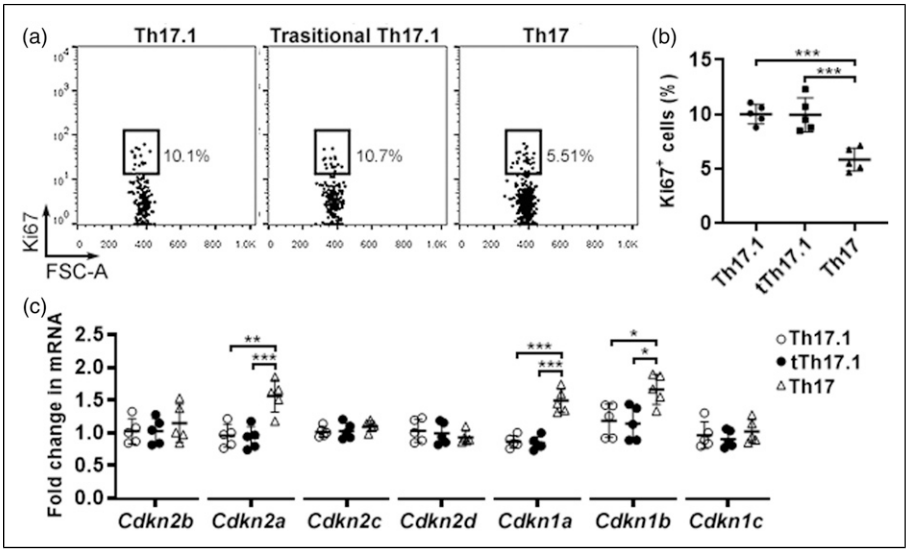

Figure 5. Proliferation of Th17.1 cells ($R3^+R4^-$ cells), transitional Th17.1 cells ($R3^+R4^+$ cells), and Th17 cells ($R3^-R4^+$ cells). (A) Representative dot plots showing Ki67 staining of indicated subsets. (B) The proportions of $Ki67^+$ cells in indicated subsets. tTh17.1: Transitional Th17.1 cells. (C) mRNA levels of indicated CDK inhibitors in the subsets. $N = 5$. *: $p < .05$. **: $p < .01$. ***: $p < .001$.

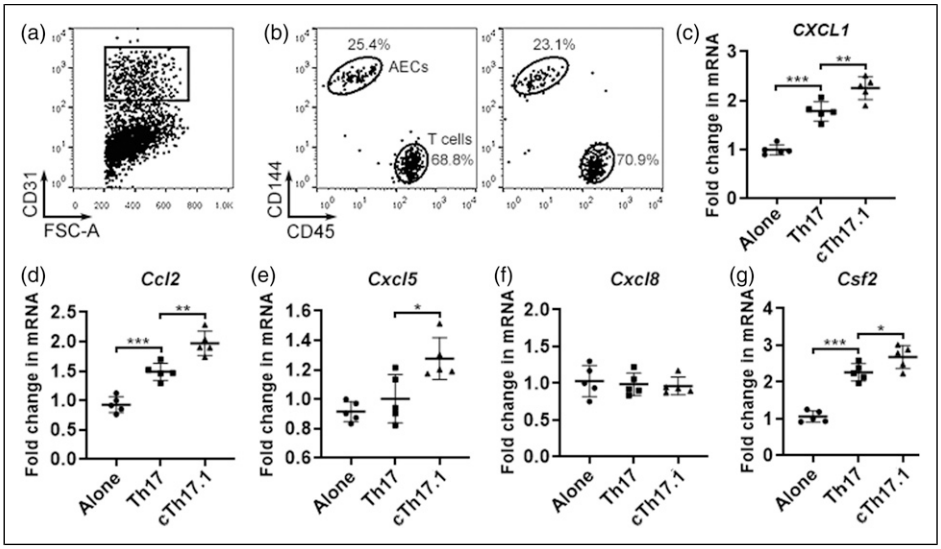

Figure 6. Effects of Th17 and combined Th17.1 cells on AECs. (A) Representative dot plots showing $CD31^+$ AECs before sorting. (B) Representative dot plots showing $CD144^+$ AECs and $CD45^+$ T cells after co-culture. (C to G) mRNA levels of indicated chemokines and GM-CSF in AECs after co-culture with Th17 or combined Th17.1 cells. Alone: AECs cultured alone. Th17: AECs co-cultured with Th17 cells. cTh17.1: AECs co-cultured with combined Th17.1 cells. $N = 5$. *: $p < .05$. **: $p < .01$. ***: $p < .001$.

expression of CXCR3 and CCR4 was differential on aortic $IL\text{-}17A^+CD4^+$ T cells and indicated different subsets. CXCR3 is expressed by Th1 cells but not by Th17 cells.[23] However, Th17.1 cells, which might be derived from Th17 cells, up-regulate CXCR3 on their surface and acquire other Th1 features such as the expression of T-bet and IFN-γ.[23,24] CCR4 is considered to be expressed by Th17 cells but not by Th1 cells.[25] Th17.1 cells lose CCR4 on their surface, demonstrating another Th1 feature.[26] Therefore, our findings are consistent with previous studies, implying that Th17.1 cells in atherosclerotic aortas might possess a similar phenotype to Th17.1 cells found in other pathological conditions.

Notably, aortic $IL\text{-}17A^+CD4^+RE^+200^+R3^+R4^-$ T cells, that is, Th17.1 cells, expressed higher T-bet and IFN-γ than $IL\text{-}17A^+CD4^+RE^+200^+R3^-R4^+$ T cells (Th17 cells), further confirming the identity of Th17.1 cells. However, the factors responsible for the generation of aortic Th17.1 cells remain unknown. Several cytokines or inflammatory mediators, including IL-1β, IL-23, prostaglandin E2 (PGE2), and TNF-α, may induce the polarization of Th17 cells toward Th17.1 cells.[23] Interestingly, these factors are present in atherosclerotic lesions,[27-31] perhaps constituting a microenvironment favorable for Th17.1 differentiation.

Based on the phenotype of aortic $IL\text{-}17A^+CD4^+$ T cells, we tried to discriminate viable aortic Th17 and Th17.1 cells by detecting the above-mentioned surface markers and avoiding intracellular cytokine staining. We successfully discerned three $CD4^+$ T subpopulations featuring Th17 and Th17.1 cells, respectively. Of note, both $CD4^+RE^+200^+R3^+R4^-$ T cells and $CD4^+RE^+200^+R3^+R4^+$ T cells expressed relatively high T-bet, suggesting their Th17.1 identity. However, the former produced more IFN-γ and TNF-α than the latter, implying that the former subset might be mature Th17.1 cells, whereas the latter subset was transitional Th17.1 cells. In the future, the two subsets should be subjected to transcriptomic profiling to unveil the molecular mechanisms underlying their functions. Meanwhile, $CD4^+RE^+200^+R3^-R4^+$ cells were likely classical Th17 cells.

Another interesting finding is that Th17.1 cells seemed to be more proliferative than Th17 cells. This is consistent with previous research showing faster proliferation of Th1 cells and Th17.1 cells relative to Th17 cells.[32] However, Th17.1 cells were still a minor subset in IL-17A-expressing T cells regardless of their faster expansion. This raises the possibility that Th17.1 cells might completely lose IL-17A expression and become Th1 cells. Indeed, the transition from Th17 cells to $IL\text{-}17^-IFN\text{-}\gamma^+$ Th1-like cells (sometimes termed ex-Th17 or nonclassical Th1) has been reported.[33,34] In the future, the lineage tracing study using IL-17A-EGFP and IFN-γ-RFP transgenic mice could reveal the fate of Th17 and Th17.1 cells in atherosclerosis.

Aortic Th17 cells expressed more p16 INK4A (encoded by *Cdkn2a*), p21 WAF1/Cip1 (encoded by *Cdkn1a*), and p27 KIP1 (encoded by *Cdkn1b*) than aortic Th17.1 cells. P16 INK4a inhibits CDK4 and CDK6 to block cell cycle progression from phase G1 to phase S.[35] p21 WAF1/Cip1 inhibits CDK1, 2, 4, and 6 to cause cell cycle arrest during G1 and S phases.[36] p27 KIP1 primarily suppresses CDK2 to stop the cell cycle at phase G1.[37] As a result, p16 INK4A blocks G1 to S transition in stimulated

T cells.[38] p21 WAF1/Cip1 inhibits activated/memory T cell expansion.[39] p27 KIP1 prevents T cell proliferation.[40] Therefore, these proteins might slow down Th17 expansion and contribute to the decrease of Th17 cells (i.e., the $R3^{-}RE^{high}$ subset) in total IL-17A-expressing T cells as shown in Figure 2(D).

Th17 cells can boost inflammatory response and foster atherosclerosis progression.[4] Th17.1 cells play crucial roles in the pathogenesis of inflammatory bowel disease, multiple sclerosis, and rheumatoid arthritis.[41] According to our data, aortic Th17.1 cells and transitional Th17.1 cells produce IFN-γ and TNF-α. IFN-γ is localized in atherosclerotic lesions to recruit inflammatory cells by inducing the expression of adhesion molecules in ECs during the early stages of atherosclerosis.[42,43] IFN-γ also induces CCL2 expression in atherosclerotic lesions.[44,45] Moreover, IFN-γ contributes to foam cell formation and reduces plaque stability.[43] TNF-α promotes inflammatory cell recruitment through up-regulating adhesion molecules, CXCL1, CCL2, and GM-CSF in endothelium.[46–49] Therefore, aortic Th17.1 cells could up-regulate chemokines and adhesion molecules to exacerbate aortic inflammation. Our research indicated that aortic Th17.1 cells plus transitional Th17.1 cells were more capable of inducing CXCL1, CCL2, CXCL5, and GM-CSF expression in AECs than Th17 cells, implying that Th17.1 cells and transitional Th17.1 cells could be more pathogenic than Th17 cells in recruiting inflammatory cells. At the early stage of atherosclerosis, Th17.1 cells are absent or minor in the atherosclerotic aorta (as evidenced in Figure 2), so Th17 cells play a significant role in atherosclerosis progression. However, over time, Th17.1 cells accumulate in the aorta and possibly co-exist with Th17 cells in atherosclerotic lesions. At the late stage, aortic Th17.1 cells might work together with Th17 cells to exacerbate aortic inflammation and promote the formation of atherosclerotic lesions.

The limitations of this study include the following: (1) The origin and the fate of aortic Th17, Th17.1, and transitional Th17.1 cells remain unclear. Future lineage tracing studies using genetically modified mouse strains might answer these questions. (2) The locations of the three subsets are not determined. Whether they are in atherosclerotic lesions and their potential interactions with other cell types should be investigated in aorta sections in the future. (3) Due to the limited numbers of these subsets, their pathogenicity has not been evaluated in vivo. In vitro expansion and adoptive transfer of aortic Th17 and Th17.1 cells could be conducted to determine their pathogenicity in the future.

Conclusion

According to the present findings, our study reveals the presence of aortic Th17.1 cells and tested their effect on the AECs. The data exhibit the presence of Th17, Th17.1, and transitional Th17.1 cells in the atherosclerotic aorta. Th17.1 cells and transitional Th17.1 cells were more proliferative than Th17 cells. Compared with Th17 cells, Th17.1 and transitional Th17.1 cells induced higher expression of pro-inflammatory chemokines and GM-CSF in AECs. Our study sheds light on the heterogeneity of aortic Th17 subsets in atherosclerosis.

Author's contributions

All authors contributed to the study. Research design and manuscript writing were performed by Xiaofang Xiong. The animal model was established by Zheng Yan and Wei Jiang. Flow cytometry analysis was conducted by Guizhen Lin and Lei Zhang. Real-time RT-PCR was performed by Beibei Wu. In vitro cell culture was carried out by Dongsheng Li.

Declaration of conflicting interests

The author(s) declared no potential conflicts of interest with respect to the research, authorship, and/or publication of this article.

Funding

The author(s) disclosed receipt of the following financial support for the research, authorship, and/or publication of this article: This work was supported by the Key Program of the Wuhan Municipal Health and Family Planning Commission Foundation (Grant # WX15A03).

Data availability

The data that support the findings of this study are available from the corresponding author, Dr. Xiaofang Xiong, upon reasonable request.

Ethics approval

Ethical approval for this study was obtained from the Wuhan University Animal Care and Use Committee (APPROVAL ID: 202,025,734).

Animal welfare

The present study followed international, national, and/or institutional guidelines for humane animal treatment and complied with relevant legislation.

ORCID iD

Xiaofang Xiong https://orcid.org/0000-0001-9039-5576

Supplemental Material

Supplemental material for this article is available online.

References

1. Markin AM, Sobenin IA, Grechko AV, et al. (2020) Cellular mechanisms of human atherogenesis: focus on chronification

of inflammation and mitochondrial mutations. *Front Pharmacol* 11: 642–2020. DOI: 10.3389/fphar.2020.00642.
2. Wolf D and Ley K (2019) Immunity and inflammation in atherosclerosis. *Circ Res* 124: 315–327. DOI: 10.1161/CIRCRESAHA.118.313591.
3. Taleb S, Tedgui A and Mallat Z (2015) IL-17 and Th17 cells in atherosclerosis: subtle and contextual roles. *Arterioscler Thromb Vasc Biol* 35: 258–264. DOI: 10.1161/ATVBAHA.114.303567.
4. Wang Y, Li W, Zhao T, et al. (2021) Interleukin-17-producing CD4(+) T cells promote inflammatory response and foster disease progression in hyperlipidemic patients and atherosclerotic mice. *Front Cardiovasc Med* 8: 667768–672021. DOI: 10.3389/fcvm.2021.667768.
5. Brauner S, Jiang X, Thorlacius GE, et al. (2018) Augmented Th17 differentiation in Trim21 deficiency promotes a stable phenotype of atherosclerotic plaques with high collagen content. *Cardiovasc Res* 114: 158–167. DOI: 10.1093/cvr/cvx181.
6. Gao Q, Jiang Y, Ma T, et al. (2010) A critical function of Th17 proinflammatory cells in the development of atherosclerotic plaque in mice. *J Immunol* 185: 5820–5827. DOI: 10.4049/jimmunol.1000116.
7. Gistera A, Robertson AK, Andersson J, et al. (2013) Transforming growth factor-beta signaling in T cells promotes stabilization of atherosclerotic plaques through an interleukin-17-dependent pathway. *Sci Transl Med* 5: 196ra100. DOI: 10.1126/scitranslmed.3006133.
8. Bystrom J, Clanchy FIL, Taher TE, et al. (2019) Functional and phenotypic heterogeneity of Th17 cells in health and disease. *Eur J Clin Invest* 49: e13032. DOI: 10.1111/eci.13032.
9. Yang P, Qian FY, Zhang MF, et al. (2019) Th17 cell pathogenicity and plasticity in rheumatoid arthritis. *J Leukoc Biol* 106: 1233–1240. DOI: 10.1002/JLB.4RU0619-197R.
10. Halim L, Romano M, McGregor R, et al. (2017) An atlas of human regulatory T helper-like cells reveals features of Th2-like tregs that support a tumorigenic environment. *Cell Rep* 20: 757–770. DOI: 10.1016/j.celrep.2017.06.079.
11. Wang C, Kang SG, Lee J, et al. (2009) The roles of CCR6 in migration of Th17 cells and regulation of effector T-cell balance in the gut. *Mucosal Immunol* 2: 173–183. DOI: 10.1038/mi.2008.84.
12. Mony JT, Khorooshi R and Owens T (2014) Chemokine receptor expression by inflammatory T cells in EAE. *Front Cell Neurosci* 8: 187. DOI: 10.3389/fncel.2014.00187.
13. Wacleche VS, Goulet JP, Gosselin A, et al. (2016) New insights into the heterogeneity of Th17 subsets contributing to HIV-1 persistence during antiretroviral therapy. *Retrovirology* 13: 59. DOI: 10.1186/s12977-016-0293-6.
14. Jiang YP, Peng YQ, Wang L, et al. (2022) RNA-sequencing identifies differentially expressed genes in T helper 17 cells in peritoneal fluid of patients with endometriosis. *J Reprod Immunol* 149: 103453. DOI: 10.1016/j.jri.2021.103453.
15. Chang SH, Reynolds JM, Pappu BP, et al. (2011) Interleukin-17C promotes Th17 cell responses and autoimmune disease via interleukin-17 receptor E. *Immunity* 35: 611–621. DOI: 10.1016/j.immuni.2011.09.010.
16. Nies JF and Panzer U (2020) IL-17C/IL-17RE: emergence of a unique axis in TH17 biology. *Front Immunol* 11: 341–2020. DOI: 10.3389/fimmu.2020.
17. Wang J, Gong J, Yang Q, et al. (2022) Interleukin-17 receptor E and C-C motif chemokine receptor 10 identify heterogeneous T helper 17 subsets in a mouse dry eye disease model. *Am J Pathol* 192: 332–343. DOI: 10.1016/j.ajpath.2021.10.021.
18. Christine Goetz AG and Bonnevier J. (2020). Identification of Novel Cell Surface Markers on Mouse and Human Th17 Cells. (accessed June 13, 2022) https://www.rndsystems.com/resources/posters/identification-novel-cell-surface-markers-mouse-and-human-th17-cells
19. MatthewButcher JMH, Ley K, Galkina E, et al. (2011) Flow cytometry analysis of immune cells within murine aortas. *JoVE* 53: 2848. DOI: 10.3791/2848.
20. Breanne N, Gjurich PLTM, V Galkina E, et al. (2015) Flow cytometric analysis of immune cells within murine aorta. *Methods Mol Biol* 1339: 161–175. DOI: 10.1007/978-1-4939-2929-0_11.
21. Fujie H, Niu K, Ohba M, et al. (2012) A distinct regulatory role of Th17 cytokines IL-17A and IL-17F in chemokine secretion from lung microvascular endothelial cells. *Inflammation* 35: 1119–1131. DOI: 10.1007/s10753-011-9419-0.
22. Wojkowska DW, Szpakowski P and Glabinski A (2017) Interleukin 17A promotes lymphocytes adhesion and induces CCL2 and CXCL1 release from brain endothelial cells. *Int J Mol Sci* 18: 1000. DOI: 10.3390/ijms18051000.
23. van Hamburg JP and Tas SW (2018) Molecular mechanisms underpinning T helper 17 cell heterogeneity and functions in rheumatoid arthritis. *J Autoimmun* 87: 69–81. DOI: 10.1016/j.jaut.2017.12.006.
24. Bailey SR, Nelson MH, Himes RA, et al. (2014) Th17 cells in cancer: the ultimate identity crisis. *Front Immunol* 5: 276–2014. DOI: 10.3389/fimmu.2014.00276.
25. Chatzileontiadou DSM, Sloane H, Nguyen AT, et al. (2020) The many faces of CD4(+) T cells: immunological and structural characteristics. *Int J Mol Sci* 22: 2020. DOI: 10.3390/ijms22010073.
26. Wacleche VS, Landay A, Routy JP, et al. (2017) The Th17 lineage: from barrier surfaces homeostasis to autoimmunity, cancer, and HIV-1 pathogenesis. *Viruses* 9: 303. DOI: 10.3390/v9100303.
27. Sterpetti AV (2020) Inflammatory cytokines and atherosclerotic plaque progression. Therapeutic implications. *Curr Atherosclerosis Rep* 22: 75. DOI: 10.1007/s11883-020-00891-3.
28. Liu W, Chang C, Hu H, et al. (2018) Interleukin-23: a new atherosclerosis target. *J Interferon Cytokine Res* 38: 440–444. DOI: 10.1089/jir.2018.0006.

29. Gross S, Tilly P, Hentsch D, et al. (2007) Vascular wall-produced prostaglandin E2 exacerbates arterial thrombosis and atherothrombosis through platelet EP3 receptors. *J Exp Med* 204: 311–320. DOI: 10.1084/jem.20061617.
30. Gomez I, Foudi N, Longrois D, et al. (2013) The role of prostaglandin E2 in human vascular inflammation. *Prostaglandins Leukot Essent Fatty Acids* 89: 55–63. DOI: 10.1016/j.plefa.2013.04.004.
31. Boesten LS, Zadelaar AS, van Nieuwkoop A, et al. (2005) Tumor necrosis factor-alpha promotes atherosclerotic lesion progression in APOE*3-Leiden transgenic mice. *Cardiovasc Res* 66: 179–185. DOI: 10.1016/j.cardiores.2005.01.001.
32. Basdeo SA, Cluxton D, Sulaimani J, et al. (2017) Ex-Th17 (Nonclassical Th1) cells are functionally distinct from classical Th1 and Th17 cells and are not constrained by regulatory T cells. *J Immunol* 198: 2249–2259. DOI: 10.4049/jimmunol.1600737.
33. Lee YK, Mukasa R, Hatton RD, et al. (2009) Developmental plasticity of Th17 and treg cells. *Curr Opin Immunol* 21: 274–280. DOI: 10.1016/j.coi.2009.05.021.
34. Annunziato F, Cosmi L, Liotta F, et al. (2012) Defining the human T helper 17 cell phenotype. *Trends Immunol* 33: 505–512. DOI: 10.1016/j.it.2012.05.004.
35. Russo D, Di Crescenzo RM, Broggi G, et al. (2020) Expression of P16INK4a in uveal melanoma: new perspectives. *Front Oncol* 10: 562074. DOI: 10.3389/fonc.2020.562074.
36. Al Bitar S and Gali-Muhtasib H (2019) The role of the cyclin dependent kinase inhibitor p21(cip1/waf1) in targeting cancer: molecular mechanisms and novel therapeutics. *Cancers* 11: 1475. DOI: 10.3390/cancers11101475.
37. Bencivenga D, Stampone E, Roberti D, et al. (2021) p27(Kip1), an intrinsically unstructured protein with scaffold properties. *Cells* 10: 2254. DOI: 10.3390/cells10092254.
38. Janelle V, Neault M, Lebel ME, et al. (2021) p16(INK4a) regulates cellular senescence in PD-1-expressing human T cells. *Front Immunol* 12: 698565. DOI: 10.3389/fimmu.2021.698565.
39. Arias CF, Ballesteros-Tato A, Garcia MI, et al. (2007) p21CIP1/WAF1 controls proliferation of activated/memory T cells and affects homeostasis and memory T cell responses. *J Immunol* 178: 2296–2306. DOI: 10.4049/jimmunol.178.4.2296.
40. Tsukiyama T, Ishida N, Shirane M, et al. (2001) Down-regulation of p27Kip1 expression is required for development and function of T cells. *J Immunol* 166: 304–312. DOI: 10.4049/jimmunol.166.1.304.
41. Kamali AN, Noorbakhsh SM, Hamedifar H, et al. (2019) A role for Th1-like Th17 cells in the pathogenesis of inflammatory and autoimmune disorders. *Mol Immunol* 105: 107–115. DOI: 10.1016/j.molimm.2018.11.015.
42. Gupta S, Pablo AM, Jiang X, et al. (1997) IFN-gamma potentiates atherosclerosis in ApoE knock-out mice. *J Clin Invest* 99: 2752–2761. DOI: 10.1172/JCI119465.
43. Moss JW and Ramji DP (2015) Interferon-gamma: promising therapeutic target in atherosclerosis. *World J Exp Med* 5: 154–159. DOI: 10.5493/wjem.v5.i3.154.
44. Charo IF and Taubman MB (2004) Chemokines in the pathogenesis of vascular disease. *Circ Res* 95: 858–866. DOI: 10.1161/01.RES.0000146672.10582.17.
45. Valente AJ, Xie JF, Abramova MA, et al. (1998) A complex element regulates IFN-gamma-stimulated monocyte chemoattractant protein-1 gene transcription. *J Immunol* 161: 3719–3728.
46. Tousoulis D, Oikonomou E, Economou EK, et al. (2016) Inflammatory cytokines in atherosclerosis: current therapeutic approaches. *Eur Heart J* 37: 1723–1732. DOI: 10.1093/eurheartj/ehv759.
47. Lo HM, Lai TH, Li CH, et al. (2014) TNF-alpha induces CXCL1 chemokine expression and release in human vascular endothelial cells in vitro via two distinct signaling pathways. *Acta Pharmacol Sin* 35: 339–350. DOI: 10.1038/aps.2013.182.
48. Murao K, Ohyama T, Imachi H, et al. (2000) TNF-alpha stimulation of MCP-1 expression is mediated by the Akt/PKB signal transduction pathway in vascular endothelial cells. *Biochem Biophys Res Commun* 276: 791–796. DOI: 10.1006/bbrc.2000.3497.
49. Takahashi M, Kitagawa S, Masuyama JI, et al. (1996) Human monocyte-endothelial cell interaction induces synthesis of granulocyte-macrophage colony-stimulating factor. *Circulation* 93: 1185–1193. DOI: 10.1161/01.cir.93.6.1185.